UCST-Type Polymer Capsules Formed by Interfacial Complexation

Lucas Sixdenier, Amélie Augé, Yue Zhao, Emmanuelle Marie, Christophe C. Tribet

UCST-Type Polymer Capsules Formed by Interfacial Complexation.

Lucas Sixdenier,[†] Amélie Augé,[‖,] Yue Zhao,[‖] Emmanuelle Marie,[†] and Christophe Tribet*[,†]

[†]P.A.S.T.E.U.R., Département de chimie, École Normale Supérieure, PSL University, Sorbonne Université, CNRS, 75005 Paris, France

[‖]Département de chimie, Université de Sherbrooke, Sherbrooke, Québec J1K 2R1, Canada

ABSTRACT: Formation of aqueous-core polymer capsules exhibiting an Upper Critical Solution Temperature (UCST) was achieved using surfactant-polymer interfacial complexation in water-in-oil inverse emulsions. In fluorinated oil, coulombic interactions between Krytox, an anionic oil-soluble surfactant, and a cationic poly(lysine) grafted with poly(acrylamide-co-acrylonitrile) enabled to form an adsorbed polymer shell at the surface of water droplets. The thermo-responsiveness of the polymer shell was assessed by fluorescence microscopy with and without the presence of nanoparticles, including gold particles. We show that, above the cloud point, polymers with a balanced fraction of UCST grafts form flat adlayers that (i) spontaneously entrap nanoparticles upon cooling and (ii) switch from fluid-like dynamics at high temperature to solid-like dynamics below the cloud point. This system offers a straightforward mean to prepare temperature-sensitive capsules in mild, biocompatible conditions, and to concentrate nanoparticles (including nanoheaters) in their shell.

On-demand release of pre-encapsulated chemical materials is a major topic for drug delivery or tissue engineering [1,2,3] agriculture,[4] food science or cosmetics.[5] The design of hollow polymer capsules comprising a stimuli-responsive polymer shell has enabled major progress to remotely control the release of core-encapsulated payloads.[6,7] Extensive studies on temperature-responsive polymers operating in water have been reported, likely because temperature shift by a few °C is a mild, non-toxic additive-free trigger.[8] These polymers are characterized either by a Lower or an Upper Critical Solution Temperature (LCST or UCST).[3,9,10,11] LCST polymer chains are switching from hydrophilic, soluble coils to hydrophobic collapsed globules upon heating above the LCST. UCST polymer chains exhibit the opposite behavior and are water-soluble above the UCST.[12,13]

In aqueous environment, LCST-based delivery systems have been markedly more studied than UCST ones.[14] Their implementation in drug carriers typically relies on gelation or rigidification occurring when they are heated above the LCST, combined with passive slow release (sustained delivery). To obtain heat-activated release, the implementation of LCST polymers in/on membranes of capsules is however counterintuitive, since the increase of temperature makes the chains more hydrophobic i.e. less permeable to water-soluble payloads.[15,16] In contrast, UCST polymers are obviously suitable for heat-triggered permeabilization, because they are insoluble at low temperature and can be dissolved upon heating. Although UCST is most likely observed in hydro-organic solvents,[12,17] polymers showing UCST in pure water are not rare. Several ones exhibit a thermal transition in temperature windows relevant for practical applications (typically 10-50 °C).[12,18] Yet, only a handful of UCST polymers has been implemented in hollow containers, namely polymersomes or nanovesicles. They were prepared using amphiphilic multiblock copolymers with UCST polymer blocks such as poly(acrylamide-co-acrylonitrile) (PAAMAN),[19] poly(phosphonate) with carboxylic acid side groups,[20] or PEGylated cyanophycin (a polyzwitterionic multi-L-arginyl-poly-L-aspartic acid).[21] The main drawback of these systems is the sensitivity of thermal responses to environmental features.[22] Their cloud point is in practice tuned by adjusting the polymer structure (composition, chain length, end-groups), but minor chemical degradation or effect of pH,[20] or salts made it a challenging task.[9, 22,23] Acidic or salt impurities may for instance shift the working temperature by >10 °C.[12,24] Cloud point of poly(N-acryloylglycinamide), one of the earliest non-ionic copolymers with chemically adjustable properties, shifts from 20 °C to above 100 °C when about 0.2 mol% of the monomers is hydrolysed.[25] Interactions with drug cargo can also perturb the thermal response.[26],[21]

Poly(acrylamide-co-acrylonitrile) (PAAMAN) combines the desirable properties of (i) becoming hydrophobic near room temperature, (ii) having a cloud point that can be tuned by adjusting monomer composition, and (iii) exhibiting minimal UCST shift in various aqueous environments, architectures and drug loading.[27,28] Accordingly, this copolymer was introduced recently as a robust switch for remote delivery by drug-loaded polymer assemblies including micelles,[29-32], nanoparticles,[26] or microgels.[33, 34] Nanoheater-containing PAAMAN microgels were shown to reversibly swell and shrink, possibly tuning diffusion and release of small cargoes. These systems relied on the release of a small

molecular load upon disassembly and dissolution of the polymers. For instance, antitumor efficacy have been reported with micelles of PEG-PAAMAN either delivering doxorubicin unde exposure to microwave[30] or switching on phototoxic ROS production upon photo-thermal solubilization.[31, 32] When they are loaded with nanoheaters, such as gold particles or dyes, these assemblies indeed dissolves either by exposure to light [3,33,32,26] or to magnetic fields.[35, 36] Temperature shift however could not always achieve a clean on/off switch of delivery, as (slow) release rate is often present at low temperature. This presumably depends on the contrast in hydrophobicity that can be obtained. Published examples show a slow leak, limiting effective use to short time window (< hours). In addition, loading of hydrophobilic cargoes into hydrophobic assemblies of PAAMAN has not been reported. Capsules made of a thick hydrophobic shell with an aqueous core do not suffer the same drawback. As far as we know, the formation of aqueous-core polymer microcapsules with UCST transition has never been reported.

In this work, we show a mild and biocompatible preparation of UCST-responsive hollow capsules made of a PAAMAN-containing shell surrounding an aqueous core. Our strategy is based on interfacial complexation in inverse emulsions, between an anionic surfactant and a polycation that was grafted with PAAMAN chains. We assessed in addition the capture of nanoparticles into the shell layer, as promising features for encapsulation of nanoheaters and future design of remotely controlled delivery systems. This approach extends a method previously implemented in our group for the design of LCST-type capsules based on poly(N-isopropylacrylamide) (PNIPAM).[37] Here, the polymer made of PAAMAN chains grafted on a cationic poly(lysine) (PLL) was dissolved in aqueous solution at high temperature, and emulsified in a fluorinated oil containing the anionic surfactant Krytox. A mixed surfactant:polymer layer spontaneously formed at the surface of water droplets (Fig. 1). The present work illustrates conditions enabling to obtain this layer, and assesses the thermal switch of hydrophobicity concomitant with a transition from a solid-like, impermeable shell at low temperature to a liquid-like, permeable and partially redispersed layer at high temperature.

PAAMAN chains of 15 kg/mol (dispersity 1.2) were synthesized by RAFT using a bifunctional trithiocarbonate chain transfer agent and an acrylamide/acrylonitrile molar ratio of 0.66/0.34 (see [38] and Synthesis section in Supporting Information (SI), Fig. S1). The cloud point of PAAMAN solutions reached a plateau above 10 g/L in pure water and was of ~45 °C (turbidimetry measurement, Fig. S3 and S4 in SI). To drive the non-ionic PAAMAN chains into interfacial complexation, they have been grafted on a cationic PLL backbone of 52 kg/mol by the following two-step procedure: 1) 7 mol% of the side amino groups of PLL were functionalized by grafting NHS-terminated maleimido-PEG linkers, and 2) the trithiocarbonate unit of PAAMAN chains was aminolyzed in-situ to produce thiol-terminated PAAMAN strands that reacted on the side maleimide groups by thiol-ene addition (Fig. 1A, and SI for details), yielding a PLL-g-PAAMAN comb-like copolymer with a PLL/PAAMAN weight ratio of 53/47 wt% (i.e. 6 PAAMAN strands per PLL chain of 52 kg/mol). In addition, dye-labeled polymers were prepared to visualize the distribution of the polymer in emulsion: to this aim, a fluorophore (here, rhodamine or coumarin) was covalently attached to the PLL backbone (see SI for details).

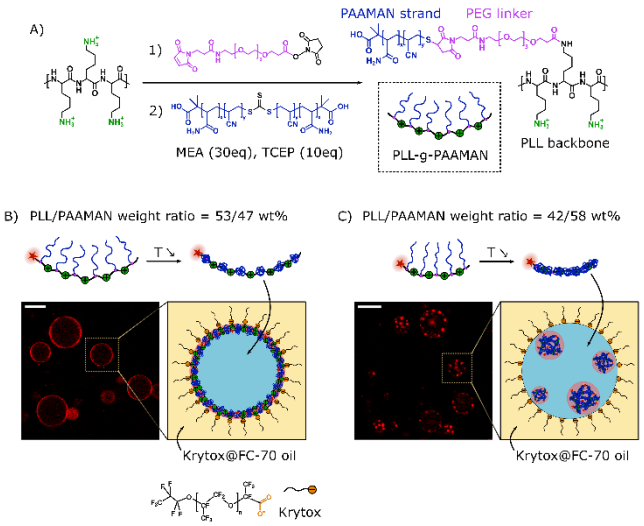

Figure 1. Preparation of polymer capsules made of poly(L-lysine)-g-poly(acrylamide-co-acrylonitrile) (PLL-g-PAAMAN). A) Synthesis procedure for the grafting of PAAMAN strands on a PLL backbone using a poly(ethylene glycol) difunctional linker. MEA = monoethanolamine, TCEP = tris(2-carboxyethyl)phosphine. B) Polymer shells formed by cooling down to 18 °C an inverse emulsion containing a rhodamine-labeled $PLL_{0.53}$-g-$PAAMAN_{0.47}$ (aqueous solution at 10 g/L in 20 mM KSCN) and initially prepared at 60 °C. The FC-70 fluorocarbon oil phase contained 0.5 g/L Krytox surfactant. C) Globular association of rhodamine-labeled $PLL_{0.42}$-g-$PAAMAN_{0.58}$ chains in the same conditions of emulsion formulation as in B). Scale bar in the confocal micrographs = 30 µm.

The cloud point of a 10 g/L PLL-g-PAAMAN solution in water was of ~ 49 °C (Fig. S3 in SI), suggesting that the grafting on PLL slightly shifted the UCST as compared to ungrafted PAAMAN. Several other effects can however affect the

cloud point. Variations by more than 10 °C were measured in the presence of salts in a 20-100 mM concentration window (Fig. S4 in SI). Of note a 10 g/L PLL-g-PAAMAN correspond to a concentration of counter ions of about 30 mM. The cloud point also varied with polymer concentration, though a plateau was reached above 10 g/L PAAMAN (Fig. S4 in SI). Finally, block copolymers containing PAAMAN blocks display cloud points that depend on the hydrophobic/philic balance of the chain.[39] Cloud point measured for PLL-g-PAAMAN copolymer (49 °C) was finally surprisingly close to the one of ungrafted PAAMAN (45 °C). Nevertheless, a temperature > 45 °C was not suitable for practical conditions of long-term microscopy observations. The transition temperature was decreased, down to ~ 37 °C, by addition of 20 mM of KSCN (Fig. S3 in SI).[27]

The aqueous phase containing PLL-g-PAAMAN polycation was emulsified above the cloud point (at 60 °C) in a continuous fluorocarbon oil (FC-70) containing the anionic surfactant (Krytox). After cooling down to ambient temperature, bright fluorescent coronas observed by confocal microscopy at the periphery of the droplets (Fig. 1B) were indicative of the formation of a polymer shell. Interestingly, the ability of PLL-g-PAAMAN to adsorb as flat layers at the interface was highly dependent on the structure of the polymer. Fig. 1C shows the case of a PLL-g-PAAMAN with a lower PLL/PAAMAN weight ratio, namely 42/58 wt% (4 PAAMAN strands per PLL chain of 22 kg/mol) that upon cooling formed globular aggregates punctuating both the core and the periphery of the droplets. Since the molar ratio of grafting onto PLL was here typically < 3 mol% the density of cationic groups in PLL-g-PAAMAN is not significantly different from PLL. Accordingly formation of coulombic complexes with Krytox is not expected to be affected by grafting. Ungrafted PAAMAN solubilized above the cloud point formed globules at low temperature that floated in droplet's core without particular adhesion to the interface (not shown). A tentative rationale of the observation of globular morphologies with a copolymer having the highest wt% of PAAMAN is accordingly that a predominance of PAAMAN in the copolymer (in terms of weight fraction) favors formation of globules that do not stick to the oil-water interface. In other terms, the % of PAAMAN can be adjusted to balance the contributions of coulombic attraction of PLL at interface and of hydrophobic globular aggregation of PAAMAN strands. Below, we report data obtained using $PLL_{0.53}$-g-$PAAMAN_{0.47}$, i.e. the copolymer yielding a flat coating of the interface.

We used fluorescence to address questions on polymer hydrophobicity, temperature sensitiveness, and fluidity that are key properties of capsule shell walls. First, the fluorescence of 8-anilinonaphtalene-1-sulfonic acid (ANS) was used as an extrinsic polarity/hydrophobicity probe.[40] In the absence of PAAMAN, ANS fluorescence was homogeneously distributed in the droplet (a reference imaging of interface covered by the hydrophilic PLL-g-PEG is shown in [37]) suggesting the absence of interaction of the probe with interfacial complexes. Fig. 2A shows confocal micrographs of a representative droplet containing PLL-g-PAAMAN (non-fluorescent) and ANS, below and above the cloud point. High fluorescence intensity at the surface of the droplets at 18 °C validates the hydrophobic nature of the polymer shell formed below the cloud point. In contrast, homogeneous fluorescence was observed at 48 °C suggesting the hydrophilicity of the environment both in the core and near the interface. Second, the fluorescence of rhodamine-labeled PLL-g-PAAMAN, used as a reporter of polymer localization, shows in Fig. 2B a bright corona at 18 °C.

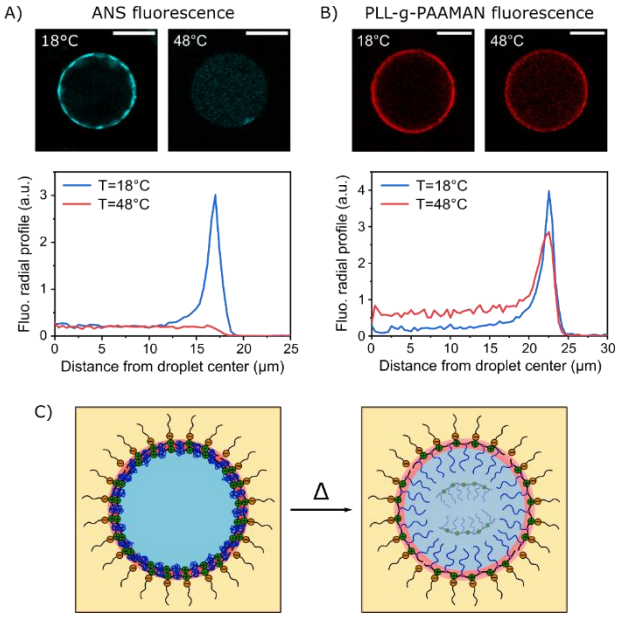

Figure 2. Thermoresponsive properties of the PLL-g-PAAMAN shells. A) Confocal micrographs and fluorescence radial profile of a representative droplet containing 10 g/L PLL-g-PAAMAN and 100 µM 8-anilinonaphtalene-1-sulfonic acid (ANS) in 20 mM KSCN, dispersed in oil containing 0.5 g/L Krytox. The emulsion was thermalized below or above the cloud point, at 18 °C or 48 °C respectively. Scale bars = 20 µm. B) Confocal micrographs and radial profiles of a representative water droplet containing 10 g/L of

rhodamine-labeled PLL-g-PAAMAN in 20 mM KSCN dispersed in oil containing 0.5 g/L Krytox at 18 °C or 48 °C.Scale bars = 20 µm. C) Schematic drawing of the increase of hydrophilicity in the adlayer, and dissolution observed upon heating.

This corona faded slightly at 48 °C, concomitantly with an increase of polymer fluorescence in the core of the drop (radial profiles in Fig. 2B). Hydrophobic-to-hydrophilic transition of PAAMAN strands likely triggers the solubilization of a fraction of the polymer chains at high temperature, as schematized in Figure 2C. When cooling the droplets down to low temperature, the polymer shell reformed reversibly as shown by i) the resurgence of fluorescence at the periphery (Fig. S5 in SI) and ii) by quantification of the polymer surface excess after and before the heating/cooling cycle (Fig. S6 in SI).

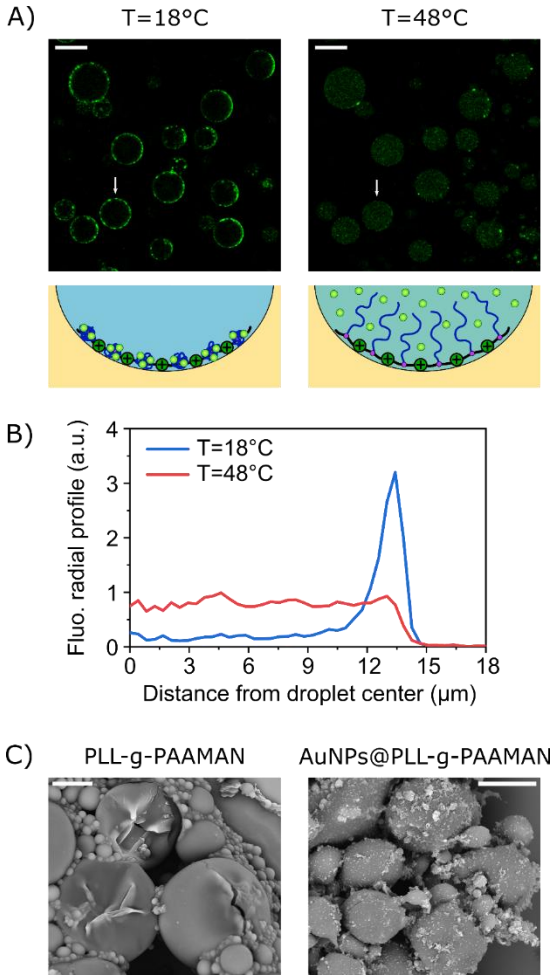

Figure 3. Formation of polymer-nanoparticles composite shells. A) *Top*: Confocal micrographs of emulsion droplets containing 10 g/L of PLL-g-PAAMAN and 0.25 g/L of NeutrAvidin-coated fluorescent nanoparticles (fluoNPS) at 18 °C and 48 °C. Scale bars = 30 µm. *Bottom*: Schematic representation of PLL-g-PAAMAN and the distribution of the fluoNPs in the droplets (Krytox molecules are not shown). B) Fluorescence radial profiles of the droplet pointed with a white arrow in the micrographs. C) SEM images of dried PLL-g-PAAMAN capsules prepared from aqueous phases with or without PVP-coated gold nanoparticles (AuNPs). Scale bars = 10 µm.

Next, we assessed the capacity of the polymer to drive a coprecipitation of nanoparticles and accordingly the formation of polymer-particles mixed adlayers. This effect may be exploited to prepare shells doped with nanoheaters such as gold particles. The capture of nanoparticles in interfacial adlayers was previously reported with PNIPAM-grafted PLL[37] and ascribed to the general propensity of PLL derivatives to adsorb onto most (anionic) particles, combined with the thermal phase transition of the PNIPAM macrografts. As a proof of concept, 50-nm NeutrAvidin-coated fluorescent nanoparticles (fluoNPs, materials in SI) were added in the aqueous phase containing PLL-g-PAAMAN prior to emulsification at 60 °C. Cooling down the emulsion to ambient temperature led to the segregation of the fluoNPs in the PLL-g-PAAMAN shell, i.e. an hydrophobic coaggregation of polymers and particles at the interface (Fig. 3A). Heating the system up to 48 °C enabled to recover soluble fluoNPs uniformly distributed in the droplet cores (Fig. 3B).

Similar experiments were done using PVP-coated gold nanoparticles (AuNPs). SEM pictures of droplets made by i) homogeneization at 60°C with or without AuNPs present in the aqueous phase, ii) cooling down to room temperature, and iii) drying at ambient air (Fig. 3C) show polydisperse capsular morphologies that were robust to drying (the

AuNPs are seen as white dots and aggregates in Fig. 3C). It cannot be ruled out however that the distribution of AuNPs is markedly affected by the drying process. To assess attraction between polymers and AuNPs, we conducted zeta potential measurements. The zeta potential of PVP-coated AuNPs shifted from -32 mV in the absence to +6 mV in the presence of PLL, indicating charge reversion of the particles, due to the binding of the cationic polymer (Fig. S7 in SI). In addition, photo-thermal dissolution of PLL-g-PAAMAN shells has been detected by irradiating AuNPs-doped emulsions at 25°C with a green laser (see Fig S8 in SI). After turning off the laser, polymer granules appeared in the targeted droplet, betraying the presence of photo-dissolved PLL-g-PAAMAN. This suggested that the cloud point was crossed due to plasmonic excitation of the AuNPs. This result is promising regarding future light-responsive delivery system based on AuNPs-doped PLL-g-PAAMAN capsules.

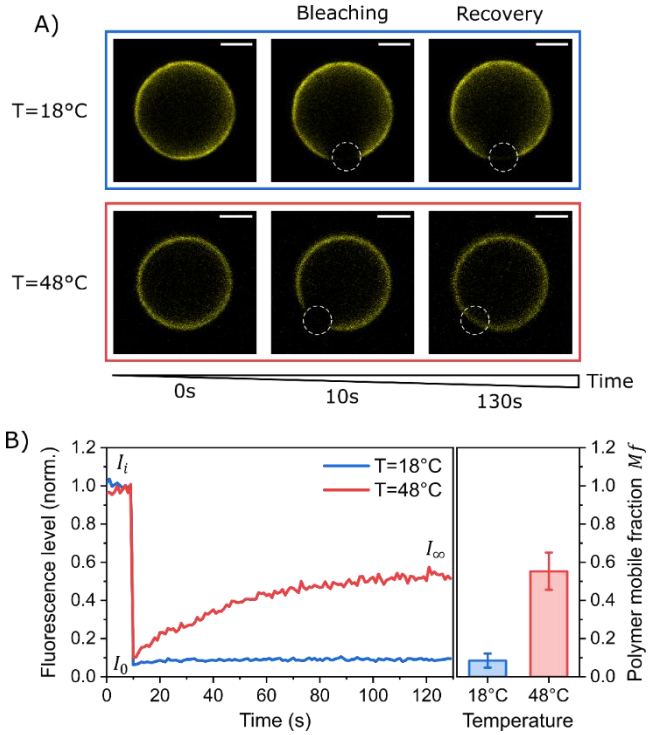

Figure 4. Fluorescence Recovery After Photobleaching on PLL-g-PAAMAN shells. A) Confocal micrographs of a representative droplet containing 10 g/L coumarin-labeled PLL-g-PAAMAN in 20 mM KSCN at 18 °C and 48 °C. Scale bars = 5 µm. B) Left: FRAP curves from the top experiments. Right: polymer mobile fraction calculated at 18 °C and 48 °C (error bars = standard deviation on 5 and 8 droplets respectively).

Changes in dynamics of the polymer shell with temperature was assessed by Fluorescence Recovery After Photobleaching (FRAP). FRAP experiments were performed on a coumarin-labeled PLL-g-PAAMAN shell (prepared in the same concentration and temperature conditions as described above) at 18 °C and 48 °C (Fig. 4A). The fraction of mobile chains within the polymer shell, M_f, was deduced from the following equation: $M_f = \frac{I_\infty - I_0}{I_i - I_0}$ where I_i is the fluorescence intensity before bleaching, I_0 the intensity just after bleaching and I_∞ the intensity at t = 2 min, assuming that a steady state was reached at this time (N.B.: to account for slow fading with observation time, intensities were normalized by the average fluorescence measured in an area away from the FRAP region ; M_f was constant for > 1min. before bleaching). A representative curve in Fig. 4B, shows almost no fluorescence recovery at 18 °C in the photobleached area. Averaging over 5 droplets indicated that the mobile chain fraction was below 10 %. Diffusion of polymer chains within the shell below the cloud point was likely frozen. In contrast at 48 °C, a partial recovery was observed at t = 2 min suggesting a fast diffusion of the chains in the polymer shell (the mobile fraction being here slightly above 50% after averaging over 8 droplets).

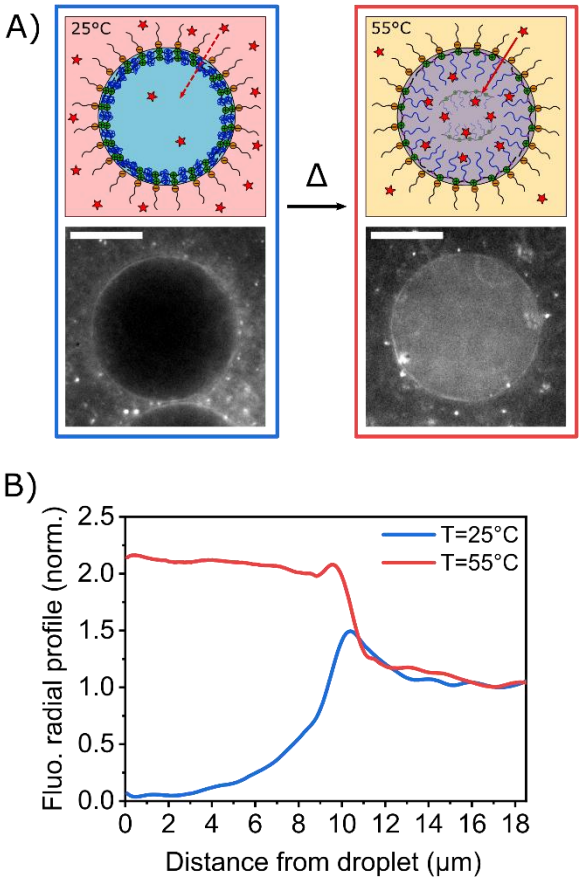

Figure 5. Permeability of PLL-g-PAAMAN shell before and after heating. A) Fluorescence micrographs of a representative droplet of 20 g/L PLL-g-PAAMAN first dispersed in fluorophore-free FC-70 oil, prior to be mixed at 25 °with (dextran-fluorescein)-containing FC-70 C. Images of the same drop taken at 25°C (left) or after heating up to 55 °C and cooling back to 25°C (right). Scale bars = 10 μm. B) Fluorescence radial profiles of the same droplet (normalized by the value in the oil phase).

Eventually, we assessed the permeability of the polymer shells to hydrophilic dextran-fluorescein (DF) of Mw 10 kg/mol. To this aim emulsions were prepared as described above (0.05% Krytox in FC-70 and no DF in the oil phase), and first equilibrated at 25°C, prior o be were mixed (50:50 v/v) with a FC-70 oil phase containing DF dissolved in micelles. Accordingly, fluorescence in the droplet cores betrays that DF has passed across the pre-formed polymer shell. In emulsions prepared with PLL-g-PEG, used as a reference hydrophilic copolymer (see method section in SI), fluorescence in the droplets was higher than in the background oil phase (Fig. S9 in SI). In contrast, the fluorescence of droplets made with PLL-g-PAAMAN was significantly lower than the background at room temperature (Fig. 5 and Fig S10). A rapid heating of the mixture up to 55 °C (< 5 min) and cooling down back to 25 °C changed the situation into brighter droplet's cores, suggesting thermally-triggered penetration of DF. Fluorescence intensities of droplets in these different conditions are illustrated in SI Fig. S10. The transition of PLL-g-PAAMAN shell into its hydrophilic state above the cloud point presumably made the shell permeable. These results are consistent with the thermal transition of the polymer shell from solid-like (insoluble) state to fluid-like, soluble state.

In conclusion, we report the formation by interfacial complexation in water-in-oil emulsion, of aqueous-core PLL-g-PAAMAN microcapsules exhibiting a UCST. The key advantages are the simplicity and biocompatibility of the formulation (emulsification in fluorinated oil above the cloud point, and cooling at room temperature), and straightforward incorporation of nanoparticles in the polymer shells with no need for specific chemistry. The hydrophobic-to-hydrophilic transition of PAAMAN chains upon heating triggers a partial dispersion of the polymer shell and a drastic change in its fluidity and permeability, switching from a solid-like impermeable state to liquid-like permeable state. In this context, the hollow structure of the capsules developed in this work may have two major advantages compared to the matrix-like systems developed so far with UCST polymers: i) the possibility to encapsulate fragile hydrophilic payloads (including biomacromolecules) in the mild aqueous core and ii) the concentration of nanoheaters within the thermo-responsive thin shell. Temperature-responsive shell combined with straightforward capture of nanoparticles is a promising route to design either photothermal delivery systems using gold nanoparticles, or magnetic hyperthermia using magnetic nanoparticles.

ASSOCIATED CONTENT

Supporting Information.
Experimental details and complementary data. This material is available free of charge via the Internet at http://pubs.acs.org.

AUTHOR INFORMATION

Corresponding Author

* Christophe Tribet – PASTEUR, Département de chimie, École normale supérieure, PSL University, Sorbonne Université, CNRS, 75005 Paris, France; Email: christophe.tribet@ens.psl.eu

Notes

The authors declare no competing financial interest.

ACKNOWLEDGMENT

LS, CT, and EM thank the following institutions and programs for the financial support: DYNAMO Laboratory of Excellence (ANR-11-LABEX-0011-01); Agence Nationale pour la Recherche (ANR-17-CE09-0007 GenCaps and ANR-17-CE09-0019 CASCADE); and Sorbonne University (Ecole Doctorale 388 scholarship). They also thank A. Yamada for the access to the SEM, J. Fattaccioli for the access to the Malvern apparatus, and J. Rieger and N. Audureau for the SEC measurement. YZ acknowledges the financial support from the Natural Sciences and Engineering Research Council of Canada (NSERC) and Fonds de recherche du Québec: Nature et technologies (FRQNT).

ABBREVIATIONS

ANS, 8-anilinonaphtalene-1-sulfonic acid; AuNPs, gold nanoparticles; DF, dextran-fluorescein; FC, fluorocarbon; fluoNPs, fluorescent NeutrAvidin-coated nanoparticles; LCST, Lower Critical Solution Temperature; MEA, monoethanolamine; PAAMAN, poly(acrylamide-co-acrylonitrile); PEG, poly(ethylene glycol); PLL, poly(L-lysine); PNIPAM, poly(N-isopropylacrylamide); RAFT, Reversible Addition-fragmentation chain Transfer; TCEP, tris(2-carboxyethyl)phosphine; UCST, Upper Critical Solution Temperature.

REFERENCES

1. Kamaly, N.; Yameen, B.; Wu, J.; Farokhzad, O. C., *Chem. Rev.* **2016,** *116* (4), 2602-2663.
2. McClements, D. J., *Adv. Coll. Interface Sci.* **2018,** *253*, 1-22.
3. Bordat, A.; Boissenot, T.; Nicolas, J.; Tsapis, N., *Adv. Drug Deliv. Rev.* **2019,** *138*, 167-192.
4. Vega-Vásquez,P.;Mosier,N.S.;Irudayaraj,J.,*Front. Bioeng. Biotechnol.* **2020,** *8*, 1-16.
5. Lee, H.; Choi, C. H.; Abbaspourrad, A.; Wesner, C.; Caggioni, M.; Zhu, T.; Weitz, D. A., *ACS Appl. Mater. Interfaces* **2016,** *8* (6), 4007-4013.
6. Esser-Kahn, A. P.; Odom, S. A.; Sottos, N. R.; White, S. R.; Moore, J. S., *Macromolecules* **2011,** *44* (14), 5539-5553.
7. Zhao, Y.; Lv, L. P.; Jiang, S.; Landfester, K.; Crespy, D., *Polym. Chem.* **2015,** *6* (23), 4197-4205.
8. Pasparakis, G.; Tsitsilianis, C., *Polymer* **2020,** *211*, 123146-123146.
9. Flemming, P.; Münch,A.S.;Fery,A.;Uhlmann,P.,*Beilstein J. Org. Chem.* **2021,***17*,2123-2163.
10. Seuring, J.; Agarwal, S., *Macromolecular Rapid Communications* **2012,** *33* (22), 1898-1920.
11. Bansal, K. K.; Upadhyay, P. K.; Saraogi, G. K.; Rosling, A.; Rosenholm, J. M., *Express Polym. Lett.* **2019,** *13* (11), 974-992.
12. Seuring, J.; Agarwal, S., *Acs Macro Letters* **2013,** *2* (7), 597-600.
13. Seuring, J.; Agarwal, S., *Macromolecules* **2012,** *45* (9), 3910-3918.
14. Halperin, A.; Kröger,M.; Winnik,F.M., *Angew. Chem. Int. Ed.* **2015,***54*(51),15342-15367.
15. Gao, H.; Yang, W.; Min, K.; Zha, L.; Wang, C.; Fu, S., *Polymer* **2005,** *46* (4), 1087-1093.
16. Schmid, A. J.; Dubbert, J.; Rudov, A. A.; Pedersen, J. S.; Lindner, P.; Karg, M.; Potemkin, I. I.; Richtering, W., *Sci. Rep.* **2016,** *6* (1), 22736.
17. Fu, W. X.; Luo, C. H.; Morin, E. A.; He, W.; Li, Z. B.; Zhao, B., *Acs Macro Letters* **2017,** *6* (2), 127-133.
18. Zhang, Z. Y.; Li, H.; Kasmi, S.; Van Herck, S.; Deswarte, K.; Lambrecht, B. N.; Hoogenboom, R.; Nuhn, L.; De Geest, B. G., *Angew. Chem. Int. Ed.* **2019,** *58* (23), 7866-7872.
19. Huang, X.; Mutlu, H.; Lin, S.; Theato, P., *Eur. Polym. J.* **2021,** *142*, 110156-110156.
20. Wolf, T.; Rheinberger, T.; Simon, J.; Wurm, F. R., *J. Am. Chem. Soc.* **2017,** *139* (32), 11064-11072.
21. Tseng, W.-C.; Fang, T.-Y.; Lin, Y.-C.; Huang, S.-J.; Huang, Y.-H., *Biomacromolecules* **2018,** *19* (12), 4585-4592.
22. Niskanen, J.; Tenhu, H., *Polym. Chem.* **2017,** *8* (1), 220-232.
23. Yu, X. R.; Liu, J. S.; Xin, Y. J.; Zhan, M. X.; Xiao, J.; Lu, L. G.; Peng, S. J., *Polym. Chem.* **2019,** *10* (47), 6423-6431.
24. Taylor, M. J.; Tomlins, P.; Sahota, T. S., Thermoresponsive Gels. *Gels* **2017,** *3* (1), 4.
25. Seuring, J.; Bayer, F. M.; Huber, K.; Agarwal, S., *Macromolecules* **2012,** *45* (1), 374-384.
26. Bordat, A.; Soliman, N.; Ben Chrait, I.; Manerlax, K.; Yagoubi, N.; Boissenot, T.; Nicolas, J.; Tsapis, N., *Eur. J. Pharm. Biopharm.* **2019,** *142*, 281-290.
27. Asadujjaman, A.; Kent, B.; Bertin, A., *Soft Matter* **2017,** *13* (3), 658-669.
28. Zhou, C.; Chen, Y.; Huang, M. J.; Ling, Y.; Yang, L. M.; Zhao, G. C.; Chen, J., *New J. Chem.* **2020,** *44* (34), 14551-14559.
29. Huang, G.; Li, H.; Feng, S.-T.; Li, X.; Tong, G.; Liu, J.; Quan, C.; Jiang, Q.; Zhang, C.; Li, Z., *Macromol. Chem. Phys.* **2015,** *216* (9), 1014-1023.
30. Li, W.; Huang, L.; Ying, X.; Jian, Y.; Hong, Y.; Hu, F.; Du, Y., *Angew. Chem. Int. Ed.* **2015,** *54* (10), 3126-3131.
31. Jiang, D.; Chen, C.; Xue, Y.; Cao, H.; Wang, C.; Yang, G.; Gao, Y.; Wang, P.; Zhang, W., *ACS Appl. Mater. Interfaces* **2019,** *11* (40), 37121-37129.
32. Deng, Y.; Käfer,F.;Chen,T.;Jin,Q.;Ji,J.;Agarwal,S., *Small* **2018,** *14* (37), 1802420.

33. Zhang, H.; Guo, S. W.; Fu, S. Y.; Zhao, Y., *Polymers* **2017,** *9* (6), 238.
34. Auge, A.; Camerel, F.; Benoist, A.; Zhao, Y., *Polym. Chem.* **2020,** *11* (23), 3863-3875.
35. Wu, L.; Zong, L.; Ni, H. H.; Liu, X. X.; Wen, W.; Feng, L.; Cao, J.; Qi, X. Y.; Ge, Y. R.; Shen, S., *Biomater. Sci.* **2019,** *7* (5), 2134-2143.
36. Huang, D.; Dai, H. T.; Tang, K. Y.; Chen, B.; Zhu, H. Z.; Chen, D. B.; Li, N.; Wang, Y. Z.; Liu, C. W.; Huang, Y. H.; Yang, J. Y.; Zhang, C.; Lin, R.; He, W. L., *Nanoscale* **2020,** *12* (38), 20002-20015.
37. Sixdenier, L.; Tribet, C.; Marie, E., *Adv. Funct. Mater.* **2021,** *2105490*.
38. Zhang, H.; Guo, S.; Fan, W.; Zhao, Y., *Macromolecules* **2016,** *49* (4), 1424-1433.
39. Zhang, H.; Tong, X.; Zhao, Y., *Langmuir* **2014,** *30* (38), 11433-11441.
40. Pramanik, P.; Ghosh, S., *J. Polym. Sci. A: Polym. Chem.* **2015,** *53* (21), 2444-2451.